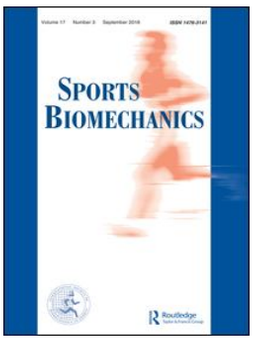

Sports Biomechanics

ISSN: (Print) (Online) Journal homepage: https://www.tandfonline.com/loi/rspb20

Numerical simulations of a swimmer's head and cap wearing different types of goggles

Daniel A. Marinho, Dennis Willemsen, Tiago M. Barbosa, António José Silva, J. Paulo Vilas-Boas, Henrique P. Neiva & Pedro Forte

To cite this article: Daniel A. Marinho, Dennis Willemsen, Tiago M. Barbosa, António José Silva, J. Paulo Vilas-Boas, Henrique P. Neiva & Pedro Forte (2021): Numerical simulations of a swimmer's head and cap wearing different types of goggles, Sports Biomechanics, DOI: 10.1080/14763141.2021.1923793

To link to this article: https://doi.org/10.1080/14763141.2021.1923793

Published online: 03 Jun 2021.

SPORTS BIOMECHANICS
https://doi.org/10.1080/14763141.2021.1923793

Routledge
Taylor & Francis Group

Numerical simulations of a swimmer's head and cap wearing different types of goggles

Daniel A. Marinho [a,f], Dennis Willemsen [b], Tiago M. Barbosa [c,f], António José Silva [d,f], J. Paulo Vilas-Boas [e], Henrique P. Neiva [a,f] and Pedro Forte [f,g]

[a]Department of Sports Sciences, University of Beira Interior, Covilhã, Portugal; [b]Department of Applied Physics, Eindhoven University of Technology, Eindhoven, Netherlands; [c]Department of Sports Sciences and Physical Education, Instituto Politécnico de Bragança, Bragança, Portugal; [d]Department of Sports Sciences, University of Trás-os-Montes and Alto Douro, Vila Real, Portugal; [e]University of Porto, Faculty of Sport (FADEUP-CIFI2D), Porto Biomechanics Laboratory (LABIOMEP), Porto, Portugal; [f]Research Center in Sports Science, Health and Human Development, Covilhã, Portugal; [g]Department of Sports Sciences, Douro Higher Institute of Educational Sciences, Penafiel, Portugal

ABSTRACT

The aim of this study was to analyse the effect of swimming goggles on swimming hydrodynamics by numerical simulations. An elite swimmer volunteered for this research. The swimmer's head was scanned both without goggles, and while wearing 3 different types of goggles (Nikko, Ankor and Swedish). Numerical simulations were conducted at 2 m/s with the Fluent code. The condition without goggles showed the highest viscous drag (1.65 N), followed by the Ankor (1.64 N), Swedish (1.63 N) and Nikko (1.62 N) goggles, respectively. The highest pressure drag was found in the situation without goggles (11.34 N), followed by the Ankor (10.87 N), Nikko (10.78 N) and Swedish (10.20 N) goggles. The condition without goggles presented the highest total drag (12.99 N), followed by the Ankor (12.52 N), Nikko (12.40 N) and Swedish (11.83 N) goggles. Thus, Swedish goggles yields the best hydrodynamics, followed by the Nikko and Ankor goggles and lastly without goggles. Thus, goggles minimise the swimmer's drag comparing to not wearing any. The design of the goggles may impose varying drag forces and therefore it is advised to use goggles at least in competition.

ARTICLE HISTORY
Received 24 September 2020
Accepted 23 April 2021

KEYWORDS
Swimming; hydrodynamics; goggles; performance; CFD; swimwear

Introduction

Swimming performance is dependent on the swimmer's propulsive and resistive forces (Barbosa et al., 2018). To improve the performance, researchers have been looking for different strategies to minimise drag (Barbosa, Morais, Marques, et al., 2015). It is possible to monitor drag forces by analytical procedures, experimental techniques and numerical simulations by computational fluid dynamics (CFD) (Marinho et al., 2009; Mollendorf et al., 2004; Naemi et al., 2010). CFD enables measuring hydrodynamic parameters with a good control of environmental features as well as controlling between and within-subject variations (Barbosa et al., 2015, 2018; Bixler & Schloder, 1996; Marinho et al. 2009). CFD has become a standard and readily available technique to

CONTACT Daniel A. Marinho dmarinho@ubi.pt

assess fluid mechanics in the past years (Marinho et al., 2009; Marinho, Barbosa, Rouboa, & Silva, 2011; Mantha et al., 2014). Numerical simulations are able to provide accurate and insightful details on the flow around the swimmer (Bixler et al., 2007). Additionally, CFD is often more affordable and less time-consuming than experimental testing (Gordon & Imbabi, 1998).

In previous CFD studies, human bodies and body segments have been used to improve the computational economy (Aritan et al., 1997; Forte et al., 2016, 2017). Simulations of anatomic segments such as the head (Forte et al., 2016, 2017), forearm (Rouboa et al., 2006) or hand (Marinho et al., 2009b) have been carried out. CFD was also employed to test sports equipment, such as helmets in aero sports (Forte et al., 2020, 2016, 2017), caps (Gatta et al., 2013; Marinho, Mantha, et al., 2011), swimsuits (Marinho et al., 2012) and paddles (Smith, 2016). All these studies provided solid evidence that equipment and its different types can affect the hydrodynamics. This happens because the object's geometry affects the fluid flow and therefore the drag force acting on the body (Forte et al., 2020b, 2020c).

Goggles are a mainstream piece of sportswear in competitive swimming. Its role is to protect the eyeballs and enable a sharper vision accuracy underwater (Morgan et al., 2008). However, as far as the authors' understanding goes, no research studying the effect of goggles on the swimmer's hydrodynamics was yet conducted. One may argue that different goggles models could impose varying amounts of drag force acting on the swimmer. Nevertheless, we failed to find a study reporting whether this is indeed the case and, in such circumstances, how much the drag increase would be. Such a study would require the selection of an analysis technique that could provide a good control of environmental conditions, besides the within-subject variability (i.e., the best way to have insight on the effect of goggles on the swimmer's hydrodynamics would be to run numerical simulations by CFD). This procedure assesses the fluid flow behaviour and provides information about drag and pressure zones (Forte et al., 2020).

The aim of this study was to analyse the effect of swimming goggles on swimming hydrodynamics by numerical simulations. It was hypothesised that the use of goggles would affect the swimmer's hydrodynamics and this would vary based on the goggles models to be worn.

Methods

Subject and scanning the model

A 30 year old elite swimmer (1.71 m height, 66 kg of body mass, 21 years of training experience, best performance of 865 FINA points) was recruited for this research. All the procedures were in accordance with the Helsinki declaration and an informed written consent was obtained beforehand. The approval was granted by the Ethics Committee of the University of Beira Interior (Portugal) under registration number R-1857-S.

The swimmer was scanned wearing a competition swimming cap. Scans were made under 4 different conditions (Figure 1): (1) not wearing goggles; (2) wearing Nikko goggles (with an oval-shape, featuring a double rim at the edges; this is the largest of all models under study); (3) wearing Ankor goggles (its main feature is the narrow height); and (4) wearing Swedish goggles (the most popular model among swimmers, the shape

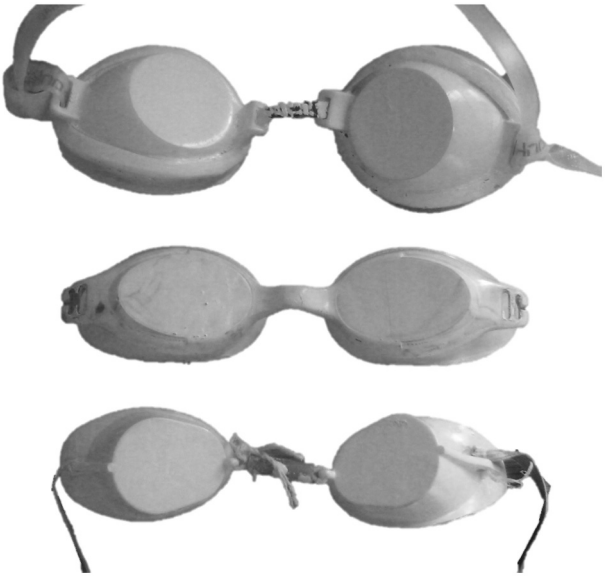

Figure 1. The Nikko, Ankor and Swedish (top to bottom) goggles.

lines closely fit the face anatomy). The goggles were painted in white to enhance the sports equipment scanning procedure and obtain a better portrait of its geometry.

The swimmer's head was scanned (Artec 3D scanner, 3D Artec TDSL (2011–08), M size type) to collect the geometry of the anatomical unit (Forte et al., 2016, 2017). The 3D scanner was fixed to a table and an anatomical unit (head, chest, neck and shoulders) spun 360º. The swimmer was sitting and scans were made under dim light to enhance the scanning procedure (Forte et al., 2016, 2017). Multiple scans from different angles, both horizontally and vertically, were made. Artec Studio Software was used to clean each scan. After aligning all the scans, the files were merged into 1 mesh (Forte et al., 2018). Upon that, a final edit consisting of filling holes, smoothing edges and applying mesh simplification was done to get the extracted geometry (Forte et al., 2018).

Subsequently, the scan files were imported into Geomagic Studio (3D Systems, USA) software. Through the use of this software, the remaining holes were filled in, noise data were deleted, and spikes and anatomical structures were smoothed (Forte et al., 2020c). After this procedure, the files were converted to points to create uniform node distances and reduce noise data. Four 3D files were created in stereolithography (Figure 2): (1) not wearing goggles (Figure 2, left above); (2) wearing Nikko goggles (Figure 2, right above); (3) wearing Ankor goggles (Figure 2, left below); and (4) wearing Swedish goggles (Figure 2, right below). Only the head was used to run the simulations. All remaining anatomical parts of the model were erased (neck, chest, shoulders and arms).

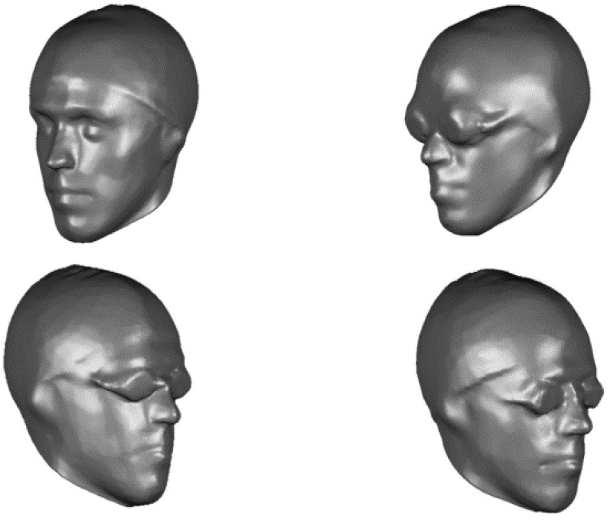

Figure 2. Three-dimensional models of swimmer's head not wearing goggles (left above), wearing Nikko goggles (right above), Ankor goggles (left below) and Swedish goggles (right below).

Boundary conditions

The swimmer's human head model resembles a sphere-like geometry. To conform to this shape, a cylindrical domain was created (radius of 0.5 m and 2.5 m length) (Moreira et al., 2006). For the mesh generation, the automatic meshing option available in the Ansys Fluent 15.0.7 commercial software was used. The automatic mesh generator implemented in the Ansys software is able to create both structured and unstructured grids of good quality. Manually creating a 3D grid with the same or even better quality would be too time-consuming. Moreover, developing a structured mesh manually can be very complex on curved and detailed anatomical geometries, such as a human face (Marinho et al., 2010).

For identical imported head geometries, 3 different grid generation techniques were tested: (1) the polyhedral meshing; (2) the tetrahedron assembly meshing; and (3) the cut cell assembly meshing. The Relevance Center settings were chosen in such a way that a sufficiently detailed grid was created for the head geometry, while still keeping acceptable computation times. A coarse relevance centre was created with polyhedral meshing and a fine relevance centre was used for both the tetrahedron and cut cell assembly meshing (Blocken et al., 2013).

The meshes were analysed by computing the skewness, orthogonal quality, number of elements and Y+ wall turbulence values (Peters, 2009). The CutCell assembly meshing method was able to generate the best quality grid. As this method creates a highly structured grid, the element count of approximately 600,000 cells was significantly lower than for the more unstructured polyhedral grids of around 1 million cells. The tetrahedron cell count was similar to that of the CutCell meshing. Also, a block-structured approach often guarantees a better quality mesh, providing more accuracy than a highly unstructured mesh (Peters, 2009).

The generated mesh was fine near the head and coarser towards the outer edges of the domain (Figure 3). This especially enables accurate flow results near the head and

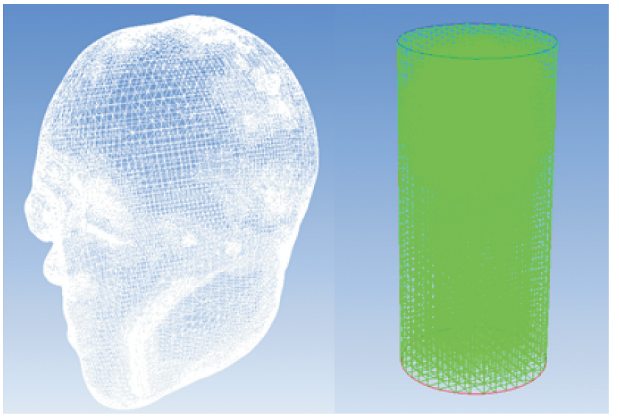

Figure 3. Fine mesh near the head (left) and coarser towards the outer edges of the domain (right).

goggles, simulating reliable boundary layers and near-surface water flows. Also, 'proximity and curvature' were selected for the grid generation. For the best quality mesh, sharp changes in the size of adjacent mesh cells should be prevented. In all cases, the 'smoothing' was set to 'high' and a programme-controlled 'inflation' setting was imposed on the mesh.

Numerical simulations

All CFD simulations were run with 3D double-precision settings. For the near-wall treatment, non-equilibrium wall functions were selected (Forte et al., 2018). These give improved predictions for fluid flows in the case of strong separation and large adverse pressure gradients compared to the standard wall-functions (Bakker, 2006). For the turbulence modelling, the viscous Realizable k-epsilon model was selected. The k-epsilon turbulence model is a 2-equation model with good predictions for turbulent flows. The model has been used successfully and extensively for industrial applications (Raiesi et al., 2011) and has shown good accuracy in modelling human swimming (Bixler et al., 2007; Bixler & Riewald, 2002; Moreira et al., 2006).

The head model without goggles presented Reynolds number of 4.14×10^7. For the model with Swedish goggles, the Re was 4.22×10^7. The model with Ankor goggles presented a Re of 4.46×10^7. Finally, the model with Nikko goggles presented a Re of 4.46×10^7. Thus, in all situations, the flow is considered turbulent.

The following boundary conditions were used (Figure 4): Cylinder top face = 'velocity inlet', normal to boundary; Cylinder bottom face = 'pressure outlet'; Cylinder side-walls = 'symmetry' ($d/dy = 0$, viscosity $v = 0$) to avoid water flow congestion; Head = 'no-slip wall' (speed $v = 0$, viscosity $v = 0$). The head model's vertex point was perpendicular with the velocity inlet face. Thus, the head angle of attack with the flow inlet velocity was 90º with an aligned head. Based on a previous study by CFD, this was considered as the best hydrodynamic position (Popa et al., 2014; Zaidi, Taiar, Fohanno, & Polidori, 2008). This aligned position presented the lowest drag in a previous study. The inlet velocity at the top of the cylinder domain was set to a steady-state flow of 2.0 m/s, representing

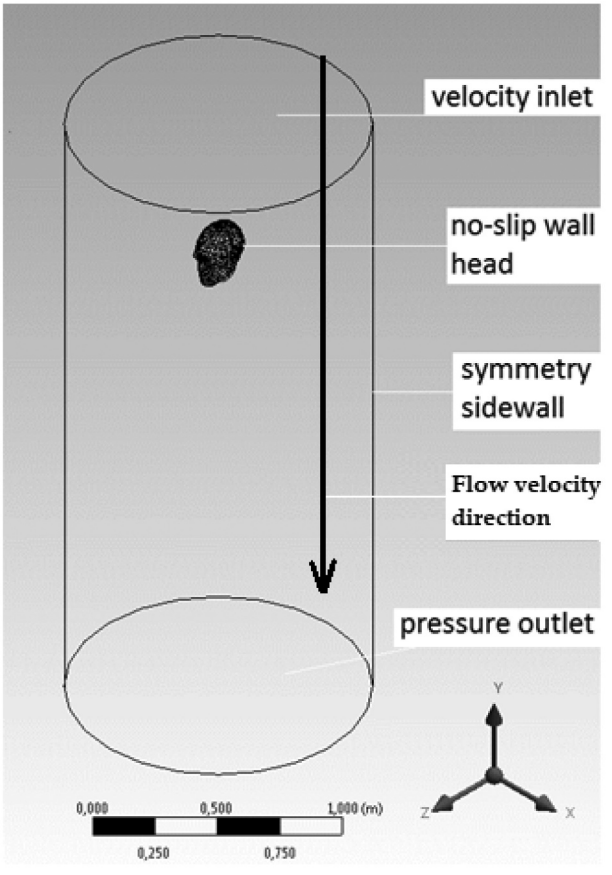

Figure 4. Boundary conditions within the entire domain geometry.

a realistic average swimming velocity in competitive short-distance swimming. Assessing different body parts, several authors have used speeds near 2 m/s that are typically used during some sets in training and racing events (Marinho et al., 2009b; Marinho, Barbosa, et al., 2011, 2012; Rouboa et al., 2006).

At the velocity inlet and pressure outlet, the turbulence intensity and length scale were set to 1% and 0.1 m. These are realistic physical values for close to standstill low turbulence water present in a swimming pool (Bixler & Riewald, 2002). The incompressible fluid in the CFD domain was given the characteristics of water (density of 998.2 kg/m^3 and dynamic viscosity of 0.001003 kg/m·s^{-1}) (Bixler & Riewald, 2002). Turbulent kinetic energy and turbulent dissipation rate were set to second-order upwind (Rouboa & Silva, 2007) and residual convergence criteria of the flow parameters were set to 10×10^{-6} for the most accurate results. Residuals of the flow velocity components in the x-, y- and z-directions were monitored. When the residual and drag values remained close to constant, showing only small fluctuations, the simulation was deemed as converged (around 1500 iterations needed).

Outcomes

Drag force

Viscous drag, pressure drag, total drag and surface area were extracted from the Ansys Fluent Software (Ansys Fluent 15.0.7, Ansys Inc., Pennsylvania, USA). The total drag is defined as

$$F_d = \frac{1}{2}\rho A C_d v^2 \tag{1}$$

where F_d is the drag force, C_d represents the drag coefficient, v is the velocity, A is the cross-section surface area and ρ is the water density (998.2 kg/m^3). It is possible to obtain the effective surface area (AC_d) by multiplying A by C_d. This variable encompasses the head surface area and the fluid flow around it.

The pressure drag (F_{dp}) and the viscous drag (F_{dv}) are given by

$$F_{dp} = \frac{1}{2}\rho A C_{dp} v^2 \tag{2}$$

$$F_{dv} = \frac{1}{2}\rho A C_{dv} v^2 \tag{3}$$

Pressure contours were also obtained from the code for qualitative analysis. These images depict the head geometry zones with higher pressure during the fluid flow.

Results

Drag

Table 1 presents the pressure, viscous and total drag, and the percentual contribution to the total drag as found in the CFD simulations. Obviously, the pressure drag values are higher than the viscous forces. The computed viscous drag force was different across all 4 models (partial differences between 1% and 2%). Not wearing goggles had the highest viscous drag (1.65 N), followed by the Ankor (1.64 N), Swedish (1.63 N) and Nikko (1.62 N) goggles, respectively.

The pressure drag force is different in the 4 studied situations (partial differences ranging from 4% to 10%). While wearing the 3 goggles models, the swimmer's head experienced less pressure drag than without goggles. The Swedish goggles showed the best hydrodynamics, followed by the Nikko and Ankor models. The condition without goggles had the largest pressure drag (11.34 N), followed by the Ankor (18.87 N), Nikko (10.78 N) and Swedish (10.20 N) goggles, respectively. A similar trend was found in the total drag force. The condition without goggles showed the lowest magnitude (12.99 N)

Table 1. Drag forces acting on the swimmer's head model.

	F_{dp} (F_d%) (N)	F_{dv} (F_d%) (N)	F_d (N)	A (m^2)
Without goggles	11.34 (87%)	1.65 (13%)	12.99	0.025
Swedish	10.20 (86%)	1.63 (14%)	11.83	0.026
Ankor	10.87 (87%)	1.64 (13%)	12.51	0.029
Nikko	10.78 (93%)	1.62 (7%)	12.40	0.029

of the total drag, followed by the Ankor (12.51 N), Nikko (12.40 N) and Swedish (11.83 N), respectively. For the effective surface area (AC_d) the same order applied.

Altogether, the Swedish goggles decreased the drag force on the head model by 9% compared to the control condition (not wearing goggles). The 2 other goggles models also decreased the drag force, but just by 5% and 4%, respectively.

Pressure maps

In all the conditions, the highest-pressure zone is located on the top of the head (Figure 5). The tip part of the nose is also a high-pressure zone. The main low-pressure zones are the eyes or goggles, nostrils and ala (borders) of the nose, and the mandible (notably mental protuberance). At these locations, water is forced to flow around curved geometries, causing negative pressure gradients and imposing a fluid acceleration.

Depending on the shape of the goggles, the surface area around the eye regions has different geometries. Curved obstacles, whether a certain type of goggles or cavity of the human eye socket, induce a forced normal acceleration of the streaming water. The curved water flows cause pressure gradients on the surface of the model. Besides

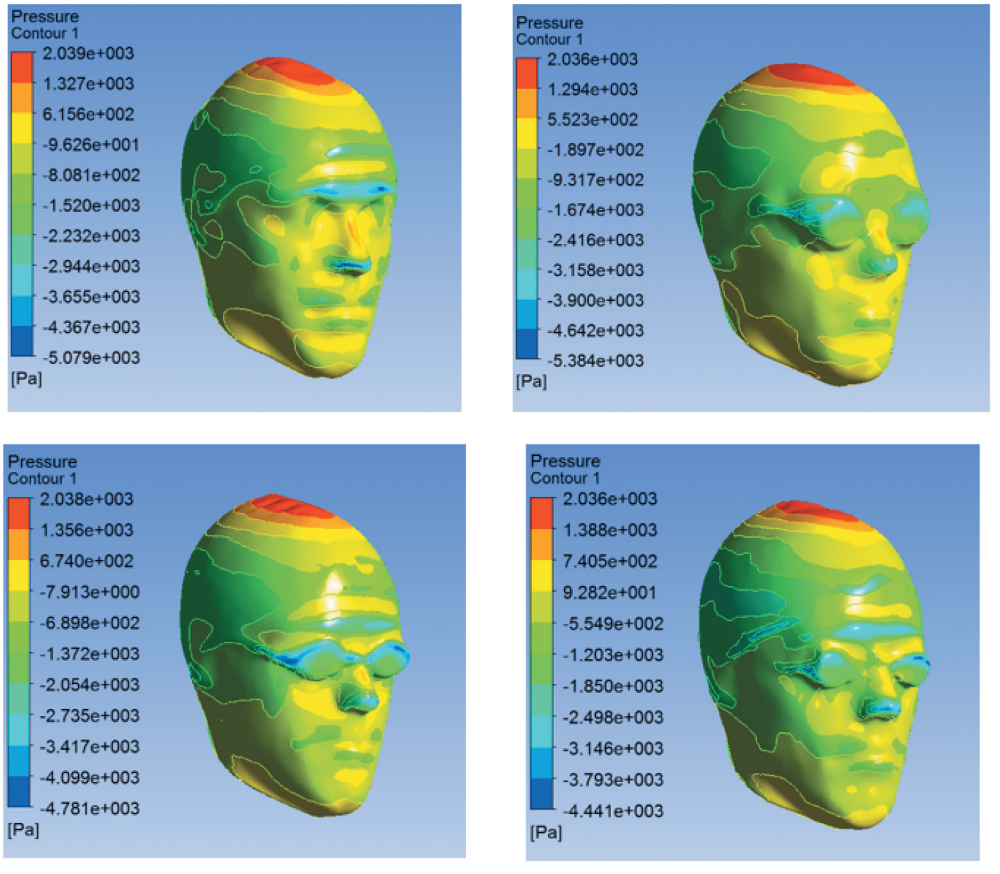

Figure 5. The pressure maps for the following situations: without goggles (left above), wearing Nikko (right above), Ankor (left below) and Swedish goggles (right below).

differences in eyepiece geometry, the goggles slightly vary the shape of the noseband, head strap and flat surface area.

Discussion and implications

The current study aimed to assess the hydrodynamic characteristics of a swimmer's head model wearing different swimming goggles. It was hypothesised that by wearing goggles the pressure, viscous and total drag change. The main results demonstrated that without goggles the swimmer's head model experiences a larger drag force than when wearing goggles. Comparing the 3 goggles models, the largest force was found while wearing the Ankor model, then with the Nikko model and the smallest force using the Swedish model.

Without goggles the head experienced a drag force of 12.99 N at 2.0 m/s, whereas with the goggles it varied between 11.83 and 12.51 N. In other studies, at 2.0 m/s, assessing the head influence position in the upper trunk, limbs and head geometry (Cortesi & Gatta, 2015) and full-body gliding position (Barbosa et al., 2018), the drag values were near 100 N. However, the authors (Barbosa et al., 2018; Cortesi & Gatta, 2015) ran the simulations to a larger body area (upper-body and full-bodied geometries), whereas in the present study, only the flow around the head was simulated, which represents only a small part of the total drag of the body during swimming. In the current study, the pressure drag contribution to the total drag at the same speed was between 86.22% and 87.29%. This is in accordance with Barbosa et al. (2018) who calculated a pressure drag contribution to the total drag of 83.14% at 2.0 m/s. The swimmer's head surface area ranged between 0.025 and 0.029 m^2. However, no study was found in the literature reporting the swimmer's head surface area. The head model without goggles had the lowest surface area (0.025 m^2), followed by the head with the Swedish goggles (0.026 m2), Niko and Ankor goggles (0.029 m^2). This increases the hydrodynamic relevance of the goggles, reducing drag to a larger surface area.

Wearing goggles reduced the total drag force exerted over the swimmer's head by 4–9%, depending on the model. The viscous drag differences were between 1% and 2%, whereas the pressure drag differences were between 4% and 10%. These results show that the pressure drag is the main factor in the drag reduction when wearing goggles. The goggles design may enhance the shape, diminishing the pressure drag by improving the water flow around the face. The goggles design and the used materials allow the water to pass over the goggles more efficiently due to its frame portions being formed by a smooth and continuous surface (Van Atta et al., 2009). The smooth surfaces of the goggles materials minimise the viscous drag (Forte et al., 2020d; Schlichting, 1979). Another concern regarding the equipment design is the depth and profile of eyepiece reduction, which allows a smoother flow from the forehead over the goggles rather than the swimmer's eyes (Van Atta et al., 2009). The design of the goggles may justify the reason why the head without goggles experienced a higher drag and lower surface area compared to the situation with the goggles.

Altogether, the goggles were found to reduce the pressure, viscous and total drag. The goggles fill in a region near the eyes (the eye cavities) which without a piece of swimwear, change the water flow, increasing the drag force. The pressure drag is caused by differences of pressure between the front and back boundaries. Upon that, as higher the magnitude differences in pressure maps in the head regions, higher the pressure drag

(Schlichting, 1979). For this specific case, the pressure drag is mainly reduced by the anterior–posterior depth profile of the goggles frames. As presented in Figure 5, the pressure is diminished by the goggles design between the head and the chin part. In the model without goggles (Figure 5) the forehead section has less pressure (blue colour) and the area around the eyes has higher pressure (yellow/light green colour); whereas with the goggles, the above part has more regions with lower pressure (blue colour), and the centre and/or the goggles below area has green colour. The viscous drag is reduced by the smooth surface of the goggles. Therefore, swimmers might wear customised goggles based on their eye depth profile.

No previous study was found assessing the head contribution to total drag. However, Mantha et al. (2014) assessed the swimmer's total drag without goggles in the gliding position and the drag was near 80 N. In our study, the differences between the model without and with the goggles are up to 1.16 N. Hence, a swimmer with a total drag of 80 N wearing the Swedish goggles (less drag imposed) may possibly reduce the drag to 78.84 N. It is expected that in a freestyle competition, and assuming that the race environment is the same as the experimental environment, for the same propulsion, the swimmer's goggles may improve the speed from 2.00 to 2.03 m/s. Thus, in a 100 m freestyle competition, it is expected that a swimmer with a total drag of 80 N and at 2 m/s may end the race in 50 s. Hence, with goggles (the Swedish goggles decrease the head drag in 1.16 N), it might be possible to improve winning time by about 0.73 s or 1% (2.00 m/s = 50.00 s; 2.03 m/s = 49.28 s) for the same propulsion. However, this performance simulation is based on a different swimmer's model (Mantha et al., 2014). Consequently, the differences may vary with different swimmers.

The following limitations in the present study should be noted: (1) only 1 head position (attack angle) was tested; (2) the effect on the full-body hydrodynamics was not assessed; (3) 1 single participant took part in this research and different eye anatomies (e.g., eye orbital depth) may vary from person to person; (4) slight differences on head geometry following 4 successive scans of the same subject with different goggles may residually affect the results.

Conclusion

Wearing goggles diminishes the drag force as compared to not wearing them. Wearing this piece of swimwear enhances the head geometry shape/form, improving the water flow over the eye orbit cavities. Among the 3 tested models, the Swedish goggles showed the least drag force, followed by the Nikko and Ankor goggles. Viscous drag was reduced due to the smoother surface of the material used to make the equipment. Pressure drag reduces the anterior–posterior depth profile around the eye orbits. A swimmer may improve the head drag with goggles in approximately 4–9%.

Disclosure statement

The authors declare that this research was independently from any industrial sponsoring and from either of the goggles manufacturers.

Funding

This work was supported by the Portuguese Foundation for Science and Technology, I.P. [UIDB04045/2020].

ORCID

Daniel A. Marinho http://orcid.org/0000-0003-2351-3047
Tiago M. Barbosa http://orcid.org/0000-0001-7071-2116
J. Paulo Vilas-Boas http://orcid.org/0000-0002-4109-2939
Henrique P. Neiva http://orcid.org/0000-0001-9283-312X
Pedro Forte http://orcid.org/0000-0003-0184-6780

References

Aritan, S., Dabnichki, P., & Bartlett, R. (1997). Program for generation of three-dimensional finite element mesh from magnetic resonance imaging scans of human limbs. *Medical Engineering & Physics*, *19*(8), 681–689. https://doi.org/10.1016/S1350-4533(97)00039-8

Bakker, A. (2006), Turbulence Models; Applied Computational Fluid Dynamics, lecture 10, Fluent Inc., Boundary Layers and Separation; Applied Computational Fluid Dynamics, lecture 11, Fluent Inc.

Barbosa, T. M., Morais, J. E., Forte, P., Neiva, H., Garrido, N. D., Marinho, D. A., & Del Alamo, J. C. (2015). A comparison of experimental and analytical procedures to measure passive drag in human swimming. *PloS One*, *10*(7), e0130868. https://doi.org/10.1371/journal.pone.0130868

Barbosa, T. M., Morais, J. E., Marques, M. C., Silva, A. J., Marinho, D. A., & Kee, Y. H. (2015). Hydrodynamic profile of young swimmers: Changes over a competitive season. *Scandinavian Journal of Medicine & Science in Sports*, *25*(2), e184–e196. https://doi.org/10.1111/sms.12281

Barbosa, T. M., Ramos, R., Silva, A. J., & Marinho, D. A. (2018). Assessment of passive drag in swimming by numerical simulation and analytical procedure. *Journal of Sports Sciences*, *36*(5), 492–498. https://doi.org/10.1080/02640414.2017.1321774

Bixler, B., Pease, D., & Fairhurst, F. (2007). The accuracy of computational fluid dynamics analysis of the passive drag of a male swimmer. *Sports Biomechanics*, *6*(1), 81–98. https://doi.org/10.1080/14763140601058581

Bixler, B., & Riewald, S. (2002). Analysis of swimmer's hand and arm in steady flow conditions using computational fluid dynamics. *Journal of Biomechanics*, *35*(5), 713–717. https://doi.org/10.1016/S0021-9290(01)00246-9

Bixler, B. S., & Schloder, M. (1996). Computational fluid dynamics: An analytical tool for the 21st century swimming scientist. *Journal of Swimming Research*, *11*, 4–22.

Blocken, B., Defraeye, T., Koninckx, E., Carmeliet, J., & Hespel, P. (2013). CFD simulations of the aerodynamic drag of two drafting cyclists. *Computers & Fluids*, *71*, 435–445. https://doi.org/10.1016/j.compfluid.2012.11.012

Cortesi, M., & Gatta, G. (2015). Effect of the swimmer's head position on passive drag. *Journal of Human Kinetics, 49,* 37. https://doi.org/10.1515/hukin-2015-0106

Forte, P., Marinho, D. A., Barbosa, T. M., & Morais, J. E. (2020). Analysis of a normal and aero helmet on an elite cyclist in the dropped position. *AIMS Biophysics*, *7*(1), 54–64. https://doi.org/10.3934/biophy.2020005

Forte, P., Marinho, D. A., Morais, J. E., Morouço, P. G., Barbosa, T. M., & Jan, Y.-K. (2018). The variations on the aerodynamics of a world-ranked wheelchair sprinter in the key-moments of the stroke cycle: A numerical simulation analysis. *PLoS ONE*, *13*(2), e0193658. https://doi.org/10.1371/journal.pone.0193658

Forte, P., Marinho, D. A., Morouço, P., Pascoal-Faria, P., & Barbosa, T. M. (2017). Comparison by computer fluid dynamics of the drag force acting upon two helmets for wheelchair racers. *AIP Conference Proceedings*, *1863*(1), 520005. https://doi.org/10.1063/1.4992669

Forte, P., Marinho, D. A., Morouço, P. G., & Barbosa, T. (2016). CFD analysis of head and helmet aerodynamic drag to wheelchair racing. *In 2016 1st International Conference on Technology and Innovation in Sports, Health and Wellbeing (TISHW)* (pp. 1–6). IEEE, Vila Real, Portugal.

Forte, P., Marinho, D. A., Nikolaidis, P. T., Knechtle, B., Barbosa, T. M., & Morais, J. E. (2020b). Analysis of cyclist's drag on the aero position using numerical simulations and analytical procedures: A case study. *International Journal of Environmental Research and Public Health*, *17*(10), 3430. https://doi.org/10.3390/ijerph17103430

Forte, P., Marinho, D. A., Silveira, R., Barbosa, T. M., & Morais, J. E. (2020d). The aerodynamics and energy cost assessment of an able-bodied cyclist and amputated models by computer fluid dynamics. *Medicina*, *56*(5), 241. https://doi.org/10.3390/medicina56050241

Forte, P., Morais, J. E., P Neiva, H., Barbosa, T. M., & Marinho, D. A. (2020c). The drag crisis phenomenon on an elite road cyclist—A preliminary numerical simulations analysis in the aero position at different speeds. *International Journal of Environmental Research and Public Health*, *17*(14), 5003. https://doi.org/10.3390/ijerph17145003

Gatta, G., Zamparo, P., & Cortesi, M. (2013). Effect of swim cap model on passive drag. *The Journal of Strength & Conditioning Research*, *27*(10), 2904–2908. https://doi.org/10.1519/JSC.0b013e318280cc3a

Gordon, R., & Imbabi, M. S. (1998). CFD simulation and experimental validation of a new closed circuit wind/water tunnel design. *Journal of Fluids Engineering*, *120*(2), 311–318. https://doi.org/10.1115/1.2820650

Mantha, V. R., Marinho, D. A., Silva, A. J., & Rouboa, A. I. (2014). The 3D CFD study of gliding swimmer on passive hydrodynamics drag. *Brazilian Archives of Biology and Technology*, *57*(2), 302–308. https://doi.org/10.1590/S1516-89132014000200020

Marinho, D., Barbosa, T., Rouboa, A., & Silva, A. (2011). The hydrodynamic study of the swimming gliding: A two-dimensional computational fluid dynamics (CFD) analysis. *Journal of Human Kinetics*, *29*(2011), 49–57. https://doi.org/10.2478/v10078-011-0039-4

Marinho, D. A., Barbosa, T. M., Kjendlie, P. L., Vilas-Boas, J. P., Alves, F. B., & Rouboa, A. I. (2009). Swimming simulation: A new tool for swimming research and practical applications. In M. Peters (Ed.), *Lecture notes in computational science and engineering–computational fluid dynamics for sport simulation* (pp. 33–62). Springer.

Marinho, D. A., Barbosa, T. M., Reis, V. M., Kjendlie, P. L., Alves, F. B., Vilas-Boas, J. P., Machado, L., Silva, A. J., & Rouboa, A. I. (2010). Swimming propulsion forces are enhanced by a small finger spread. *Journal of Applied Biomechanics*, *26*(1), 87–92. https://doi.org/10.1123/jab.26.1.87

Marinho, D. A., Mantha, V. R., Rouboa, A. I., VilasBoas, J. P., Machado, L., Barbosa, T. M., & Silva, A. J. (2011). The effect of wearing a cap on the swimmer passive drag. *Proceedings of the 29th Conference of International Society of Biomechanics in Sports* (pp. 112–113).

Marinho, D. A., Mantha, V. R., Vilas-Boas, J. P., Ramos, R. J., Machado, L., Rouboa, A. I., & Silva, A. J. (2012). Effect of wearing a swimsuit on hydrodynamic drag of swimmer. *Brazilian Archives of Biology and Technology*, *55*(6), 851–856. https://doi.org/10.1590/S1516-89132012000600007

Marinho, D. A., Rouboa, A. I., Alves, F. B., Vilas-Boas, J. P., Machado, L., Reis, V. M., & Silva, A. J. (2009b). Hydrodynamic analysis of different thumb positions in swimming. *Journal of Sports Science & Medicine*, *8*(1), 58. https://www.ncbi.nlm.nih.gov/pmc/articles/PMC3737786/

Mollendorf, J. C., Termin, A. C., Oppenheim, E. R. I. C., & Pendergast, D. R. (2004). Effect of swim suit design on passive drag. *Medicine & Science in Sports & Exercise*, *36*(6), 1029–1035 pmid: 15179173. https://doi.org/10.1249/01.MSS.0000128179.02306.57

Moreira, A., Rouboa, A., Silva, A. J., Sousa, L., Marinho, D., Alves, F., … Machado, L. (2006). Computational analysis of the turbulent flow around a cylinder. *Portuguese Journal of Sport Sciences*, *6*(Suppl. 1), 105. https://rpcd.fade.up.pt/_arquivo/artigos_soltos/vol.6_supl.1/04.poster_presentations.pdf

Morgan, W. H., Cunneen, T. S., Balaratnasingam, C., & Yu, D.-Y. (2008). Wearing swimming goggles can elevate intraocular pressure. *British Journal of Ophthalmology*, *92*(9), 1218–1221. https://doi.org/10.1136/bjo.2007.136754

Naemi, R., Easson, W. J., & Sanders, R. H. (2010). Hydrodynamic glide efficiency in swimming. *Journal of Science and Medicine in Sport*, *13*(4), 444–451 pmid: 19540161. https://doi.org/10.1016/j.jsams.2009.04.009

Peters, M. (2009), Computational Fluid Dynamics for Sport Simulation, lecture notes in computational science and engineering, Springer, 18

Popa, C. V., Arfaoui, A., Fohanno, S., Taiar, R., & Polidori, G. (2014). Influence of a postural change of the swimmer's head in hydrodynamic performances using 3D CFD. *Computer Methods in Biomechanics and Biomedical Engineering*, *17*(4), 344–351. https://doi.org/10.1080/10255842.2012.683429

Raiesi, H., Piomelli, U., & Pollard, A. (2011). Evaluation of turbulence models using direct numerical and Large-Eddy simulation data. *Journal of Fluids Engineering*, *133*(2), 193–203. https://doi.org/10.1115/1.4003425

Rouboa, A., & Silva, A. (2007). Analysis of the performance parameters of the discus throw. *Science & Sports*, *22*(1), 14–19. https://doi.org/10.1016/j.scispo.2006.09.007

Rouboa, A., Silva, A., Leal, L., Rocha, J., & Alves, F. (2006). The effect of swimmer's hand/forearm acceleration on propulsive forces generation using computational fluid dynamics. *Journal of Biomechanics*, *39*(7), 1239–1248. https://doi.org/10.1016/j.jbiomech.2005.03.012

Schlichting, H. (1979). *Boundary Layer Theory*. McGraw-Hill.

Smith, J. P. (2016). (U.S. Patent No. 9,492,712). U.S. Patent and Trademark Office.

Van Atta, D. S., Reichow, A. W., Citek, K. M., & Bruce, R. M. (2009). (U.S. Patent No. 7,475,435). U.S. Patent and Trademark Office.

Zaidi, H., Taiar, R., Fohanno, S., & Polidori, G. (2008). Analysis of the effect of swimmer's head position on swimming performance using computational fluid dynamics. *Journal of Biomechanics*, *41*(6), 1350–1358. https://doi.org/10.1016/j.jbiomech.2008.02.005